HUMAN VACCINES & IMMUNOTHERAPEUTICS
2023, VOL. 19, NO. 3, 2269790
https://doi.org/10.1080/21645515.2023.2269790

Taylor & Francis
Taylor & Francis Group

RESEARCH ARTICLE

OPEN ACCESS Check for updates

AIM2 fosters lung adenocarcinoma immune escape by modulating PD-L1 expression in tumor-associated macrophages via JAK/STAT3

Hua Ye*, Wenwen Yu*, Yunlei Li*, Xiaoqiong Bao, Yangyang Ni, Xiangxiang Chen, Yangjie Sun, Ali Chen, Weilong Zhou, and Jifa Li

Department of Respiratory and Critical Care Medicine of Affiliated Yueqing Hospital, Wenzhou Medical University, Wenzhou, China

ABSTRACT

This work was devised to discuss the effect of AIM2 on the immunosuppression of LUAD tumors, as well as its molecular mechanism. An allograft mouse model was built. Mouse macrophages were isolated and collected. The infiltration level of Mø and expression of M1 Mø, M2 Mø markers, and PD-L1 were assayed by IHC and flow cytometry. Expression levels of M1 Mø and M2 Mø marker genes and PD-L1 were detected by qPCR. The expression of proteins linked with JAK/STAT3 was tested by western blot. $CD8^+$T cells and NK cells were activated *in vitro* and co-cultured with mouse macrophages, and their cytotoxicity was detected by LDH method. The proportion of CD206+PD-L1+ cells and the activation and proliferation of $CD8^+$T cells were assayed by flow cytometry. Multicolor immunofluorescence was utilized to assay the co-localization of proteins. AIM2 demonstrated a high expression in LUAD, exhibiting a conspicuous positive correlation with the expression of the M2 Mø markers as well as PD-L1. Expression of M1 markers was upregulated after knockdown of AIM2, while M2 markers expression and PD-L1 were downregulated, and the colocalization of proteins linked with PD-L1 and M2 Mø was decreased. The infiltration and cytotoxicity of $CD8^+$T cells and NK cells increased after silencing AIM2. After the knockdown of AIM2, which was enriched in the JAK/STAT3 pathway, the phosphorylation levels of JAK1, JAK2, and STAT3 were reduced, the immune infiltration level of $CD8^+$T cells increased, and the co-localization level of PD-L1 and PD-1 dropped. The activity and proliferation level of $CD8^+$T cells were increased with the reduced PD-1 expression. AIM2 fosters M2 Mø polarization and PD-L1 expression via the JAK/STAT3 pathway. Moreover, AIM2 promotes the immune escape of LUAD via the PD-1/PD-L1 axis. Our work may blaze a trail for the clinical treatment of LUAD.

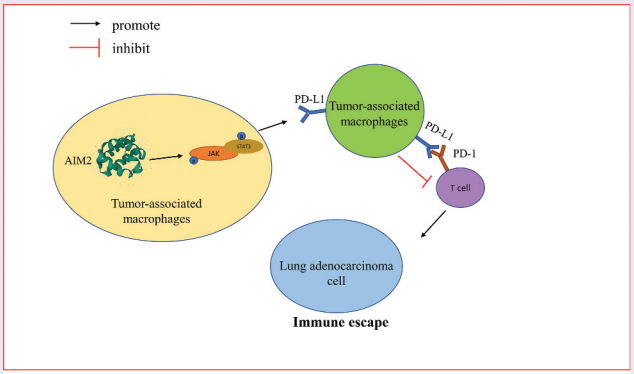

AIM2 regulates the expression of PD-L1 in tumor related macrophages through JAK/STAT3, inhibits T cell immune infiltration, and promotes lung adenocarcinoma immune escape

ARTICLE HISTORY
Received 12 May 2023
Revised 1 October 2023
Accepted 8 October 2023

KEYWORDS
AIM2; JAK/STAT3; tumor-associated macrophage; PD-L1; lung adenocarcinoma; immune escape

Introduction

Lung cancer is the major cause of cancer-related mortality worldwide. Lung adenocarcinoma (LUAD) is the most prevalent type covering around 50% of all lung cancers.[1] In spite of the ameliorations in diagnosis and treatment, the 5-year survival in individuals with LUAD is far from satisfactory (<20%).[2] Based on immune checkpoints, like programmed cell death 1 (PD-1) and programmed cell death ligand 1 (PD-L1), immunotherapies have blazed a trail for treating LUAD recently.[3] However, immune escape during treatment challenges clinical treatment. The more stable expression of PD-L1 was previously observed in tumor-associated macrophages (TAM) than in tumor cells, and in the tumor microenvironment (TME), TAM is the main source of PD-L1 expression.[4] Unfortunately, the regulatory factors of PD-L1

CONTACT Jifa Li LiJiFaLLLL@163.com Department of Respiratory and Critical Care Medicine of Affiliated Yueqing Hospital, Wenzhou Medical University, No.338 Qingyuan Road, Lecheng Town, Wenzhou 325600, China.
*These authors contributed equally.

toward TAM in LUAD remain obscure. Therefore, this work dived into the function of PD-L1 in TAM polarization and shed light on the clinical treatment of LUAD.

TAM is differentiated from monocytes derived from bone marrow into peripheral blood.[5] By stimulation of different microenvironments, macrophages (Mø) differentiate into classically activated (M1) and selectively activated (M2) subtypes.[6] Mediated by the dominance of STAT3 and STAT6, the activation of M2 Mø polarization triggers immunosuppression and fosters tumor progression,[7] and immunosuppressive factors released by M2 Mø repress T cell function and metabolism.[4] As pivotal tumor suppressor cells in tumor immunity, $CD8^+$T cells induce tumor cell apoptosis by making physical contact with malignant tumor cells and activating their intracellular signals.[3] Abnormal expression of some genes has been ascertained by current studies to repress the immune infiltration of $CD8^+$T, thus leading to tumor immune escape. For example, CD155 is overexpressed in colorectal cancer (CRC), which can reduce the proportion of cytokines secreted by $CD8^+$ cells.[8] LncRNA NEAT1 boosts anti-tumor activity of $CD8^+$T cells toward hepatocellular carcinoma by modulating miR-155/Tim-3.[9] However, the molecular mechanism leading to decreased immune infiltration of $CD8^+$T cells in LUAD remains obscure. In addition, recent studies have reported the link between AIM2 and Mø-mediated inflammatory response,[10] but whether AIM2 can affect LUAD tumor immune escape via M2 Mø remains unknown. Hence, this work dived into the mechanism of AIM2 in the polarization of M2 Mø, and offered a fresh therapeutic target for the immunotherapy of LUAD.

AIM2 belongs to the interferon (IFN)-induced PYHIN protein family.[11] AIM2 was first found in innate immune cells, like Mø and dendritic cells (DCs), with the function of sensing pathogen-linked cytosol dsDNA derived from the living host, recruiting other inflammatory components like ASC and caspase-1, and inducing caspase-dependent inflammasome formation.[12,13] Interestingly, AIM2 has been ascertained a dual role in tumors.[14] AIM2 was initially thought to be a tumor suppressor gene. For example, AIM2 represses Gli1 expression via the SMO-independent pathway and hinders CRC cells to proliferate and migrate in a Gli1-dependent manner.[15] Additionally, AIM2 plays an oncogenic role in some cancers, such as breast cancer. Knockdown of AIM2 can significantly reduce the resistance of breast cancer cells to dihydroartemisinin.[16] Furthermore, tumor immunomodulatory effects of AIM2 have also been studied. AIM2 expression in DCs in human melanoma is concerned with poor prognosis, and it plays an immunosuppressive role in TME.[17] Inoculation of AIM2-deficient DCs can improve the efficacies of adoptive T cell therapy and anti-PD-L1 immunotherapy.[17] In breast cancer and lymphoma, AIM2 is enrolled to the phagosome by FcγR signal following antibody-dependent cytotoxicity and activates phagocytized tumor DNA through the destroyed phagosome membrane, subsequently upregulating PD-L1 and IDO and causing immunosuppression.[18] To date, how AIM2 functions in the immune process of LUAD has not been elucidated. Therefore, this work dived into the impact of AIM2 on the immune process of LUAD via Mø.

We first elucidated that AIM2 fostered PD-L1 expression in TAM in LUAD, and found a new mechanism by which AIM2 promoted the immune escape of LUAD. High expression of AIM2 in LUAD promoted Mø-to-M2 phenotypic differentiation, modulated TAM polarization, and upregulated PD-L1 expression via JAK/STAT3 signaling pathway. Subsequently, we verified the immunosuppressive effect of AIM2 on LUAD by regulating PD-1/PD-L1 in TAM through cell experiments and *in vivo* experiments, hoping to blaze a trail for the clinical immunotherapy of LUAD.

Materials and methods

Bioinformatics analysis

From The Cancer Genome Atlas (TCGA) database, mRNA expression data of LUAD (normal: 59, tumor: 535) as well as relevant clinical data files were downloaded. Differentially expressed mRNAs (DEmRNAs) were obtained by edgeR differential analysis ($|\log FC|>1$, padj < 0.05). Pathway enrichment analysis of target mRNA was performed utilizing gene set enrichment analysis (GSEA) software. Pearson correlation analysis was implemented between the target gene and PD-L1 (CD274) and M2 Mø-related genes.

Establishment of the allograft model

All animal studies got the approval of the Ethics Committee of the Affiliated Yueqing Hospital of Wenzhou Medical University (YQYY202300004). LA795 cells (5×10^6 cells per mouse) were inoculated subcutaneously into the left side of 4-week-old AIM2 knockout mice (C57BL/6J-*Aim2*^{em1Cya}) (Hangzhou Hangsi Biotechnology Co., LTD., China). Tumor volume was measured every 5 days, after 25 days, mice were euthanized and weighed. Resected tumor tissue was used for histological analysis.[19]

Macrophage isolation

Primary mouse peritoneal macrophages were obtained from the peritoneal exudates of mice. The peritoneal exudate cells were washed twice with PBS solution and adjusted to 1×10^6 cells /ml in DMEM cultured for 3–4 h at 37°C and 5% CO_2. The non-adherent cells were removed by washing with warm PBS. The purity of macrophages was analyzed by flow cytometer, using a mouse macrophage marker F4/80(Abcam, UK). The adherent cells constituted more than 90% of F4/80 macrophages.[20]

In vitro *T cell and NK cell activation assay*

We conducted this experiment with reference to previous studies.[4] Simply put, the mouse spleen was ground with a syringe, rinsed with PBS, and then single-cell suspension was obtained via a 70 μm cell filter. Erythrocytes were lysed using erythrocyte lysis buffer (Biosharp, China). Spleen lymphocytes were obtained by isolating spleen cells with BALB/c mouse spleen lymphocyte isolation solution (tbdscience, China). The obtained splenic lymphocytes were kept in a complete RPMI 1640 medium. Next, for T cell activation assay, anti-CD3e (5 μg/ml; eBioscience, USA) were precoated in 96-well plates at 4°C overnight. Then, Anti-CD28 (1 μg/ml; eBioscience, USA) was introduced. For NK cell activation assay, spleen lymphocytes were stimulated with 100 U/ml IL-2 (BD Biosciences, USA) for 24 h. The activation level was subsequently determined by flow cytometry.

Cell culture

Raw264.7 cells (ATCC, USA) were kept in a complete Dulbecco's modified Eagle medium (DMEM) (Gibco, USA). LA795 cells (BLUEFBIO, China) were kept in DMEM-H with 10% fetal bovine serum. All cells were cultured in an incubator containing 5% CO_2 at 37°C. After being treated with 20 ng/mL IL-4 (NOVUS, USA), Mø produced M2 Mø. After being treated with 50 ng/mL LPS and 20 ng/mL IFN-γ (NOVUS, USA), Mø produced M1 Mø.

Cell co-culture

LUAD cells were diluted to a concentration of 1.5×10^5 cells per milliliter in high-glucose DMEM medium. The designated proportion of Mø was introduced into the RPMI 1640 medium. Subsequently, activated $CD8^+$T cells and NK cells were separately co-cultured with the processed LUAD cells in this medium at an effector-to-target (E:T) ratio of 10:1, at 37°C for 4 h. The supernatant was then collected for subsequent experiments.

For co-culture analysis, the designated proportion of Mø was introduced to the medium following T cell activation. Besides, cells were co-cultured with or without neutralizing monoclonal antibodies against PD-L1 (eBioscience, USA), PD-1 (BioXcell, USA), or IgG isotype control. Four days later, cells were examined by flow cytometry.

Cytotoxicity assay

The integrity of the cell membrane was assessed using a lactate dehydrogenase (LDH) assay kit (Beyotime, China) to determine the cytotoxicity of $CD8^+$ T cells and NK cells. In brief, cells subjected to different transfection treatments were centrifuged, and 120 µL of the supernatant was collected and transferred to a new 96-well plate. LDH release reagent was used to lyse the cells, and the absorbance was measured at 490 nm using Epoch 2 (BioTek, USA).

Cell transfection

Lipofectamine 2000 (Thermo Fisher Scientific, USA) was utilized to transfect 1 µg of sh-AIM2, oe-AIM2, and corresponding negative controls purchased from Ribobio into cells. AIM2 knockdown was achieved using shRNA constructs (AIM2: 5'-GATCCGCAAACTATCAATCAATCAAGAGATGTTTCA-GTAGTTAGTGTTTTACGTGGTG-3') and the pLKO.1 Lentivirus Particle Transduction system (Gene Chemistry, China). Cells in which AIM2 was stably knocked down were then selected with allopurinol, while empty lentiviral particles were used as a negative control. After 24 h, the next experiment was carried out. Cells were treated with 1 µM of AZD1480 (Solarbio, China).

RNA extraction and quantitative real-time polymerase chain reaction (qPCR)

Total RNA was stemmed from cells utilizing the MicroElute Total RNA Kit R6831–01 (Omega Bio-tek, USA) and then reversely transcribed into cDNA utilizing HiScript III RT SuperMix (+gDNA wiper) (vazyme, China). Amplification of cDNA was conducted by AceQ Universal SYBR qPCR Master Mix (vazyme, China). Table 1 lists the primer sequences, which were all synthesized by Sangon Biotech (China).

Western blot (WB)

RIPA lysis buffer was utilized to lyse cells, subsequently segregated by SDS-PAGE, and transferred to PVDF membranes. After being sealed in skim milk (5%) powder for 1 h at room temperature, membranes were kept with the corresponding rabbit anti-primary antibodies at 4°C overnight, then washed and kept with secondary antibody goat anti-rabbit IgG (Abcam, UK) prior to detection. The primary antibodies used in the experiments (Arg1, p-JAK1, p-JAK2, JAK1, p-STAT3, JAK2, STAT3, PD-L1) were procured from Abcam (UK). Finally, the protein signal was tested by SuperSignal West Pico PLUS chemiluminescence substrate (Thermo Fisher Scientific, USA).[21]

Immunohistochemistry (IHC) assay

Four-µm-thick sections of tumor sections were prepared and deparaffinized in xylene for 10 min. 3% H_2O_2 was utilized for immersing slides for 20 min to block endogenous peroxidase, and slides were sealed in goat serum blocking solution for half an hour. After being incubated with rabbit anti-primary antibodies overnight at 4°C, slides were incubated with secondary antibody HRP-conjugated goat anti-rabbit IgG (Abcam, UK) for half an hour at room temperature. Primary antibodies used here were: F4/80, PD-L1, iNOS, CD206, CD8, CD49b, and CD4, all purchased from Abcam (UK). IHC staining was finally examined under the microscope.

Immunofluorescence (IF) assay

Slides of tumor tissue were deparaffinized in xylene and dehydrated in the graded ethanol solution. Sections were placed at room temperature in goat serum-blocking solution

Table 1. qRT-PCR primers.

Gene	Forward Primer Sequence 5′–3′	Reverse Primer Sequence 5′–3′
Aim2	CACACTCGACGTGGCAGATAGGAC	CAGCACCGTGACAACAAGTGG
IL-12p40	ACCAGAGCAGTGAGGTCTTAGGC	TGTGAAGCAGCAGGAGCGAATG
TNF-α	GGTGCCTATGTCTCAGCCTCTT	GCCATAGAACTGATGAGAGGGAG
CD86	TTTGTGATGGCCTTCCTGCT	TGGAAACGTCGTACAGTTCTGT
Arg1	CATTGGCTTGCGAGACGTAGAC	GCTGAAGGTCTCTTCCATCACC
IL-10	CGGGAAGACAATAACTGCACCC	CGGTTAGCAGTATGTTGTCCAGC
CD206	GGGACTCTGGATTGGACTCA	CCAGGCTCTGATGATGGACT
PD-L1	AAGCCTCAGCACAGCAACTTCAG	TGTAGTCCGCACCACCGTAGC
β-actin	TGTAGTCCGCACCACCGTAGC	TGTAGTCCGCACCACCGTAGC

for 1 h. Slides were kept overnight at 4°C with the following primary rabbit anti-human antibodies for multicolor IF staining: F4/80 (Abcam, UK), PD-L1 (Abcam, UK), CD206 (Abcam, UK), Arg1 (Abcam, UK), and iNOS (Abcam, UK). The following day, slides were rinsed with phosphate-buffered saline (PBS) and stained with secondary antibody goat anti-rabbit IgG (Abcam, UK) for 1 h at room temperature. Confocal microscopy was utilized to measure multicolor IF staining.

Flow cytometry

This experiment was conducted with reference to previous studies.[4] Antibodies (F4/80, CD11b, CD206, and iNOS) were procured from Abcam (UK). Antibodies (PE-Ki-67, PE/Cy7-PD-L1, PE-IFN-γ, and APC-CD206) were bought from Biolegend (USA).

Statistical analysis

Student's t-test was utilized to analyze the mean difference. One-way analysis of variance was utilized for multiple groups followed by multiple comparisons. All data were exhibited as mean±SD. $P < .05$ was considered to denote a significant difference. All experiments were fulfilled in triplicate independently.

Results

AIM2 fosters Mø to M2-type polarization

It has been reported that AIM2 expression in the DCs of melanoma is linked with poor prognosis and plays an immunosuppressive role in melanoma microenvironment.[17] However, whether AIM2 exerts the same immune effect in LUAD is yet obscure. Therefore, to verify how AIM2 affects LUAD, we assayed the expression level of AIM2 by bioinformatics, and AIM2 was found to be significantly highly expressed in LUAD tissues (Figure 1a). To elucidate how

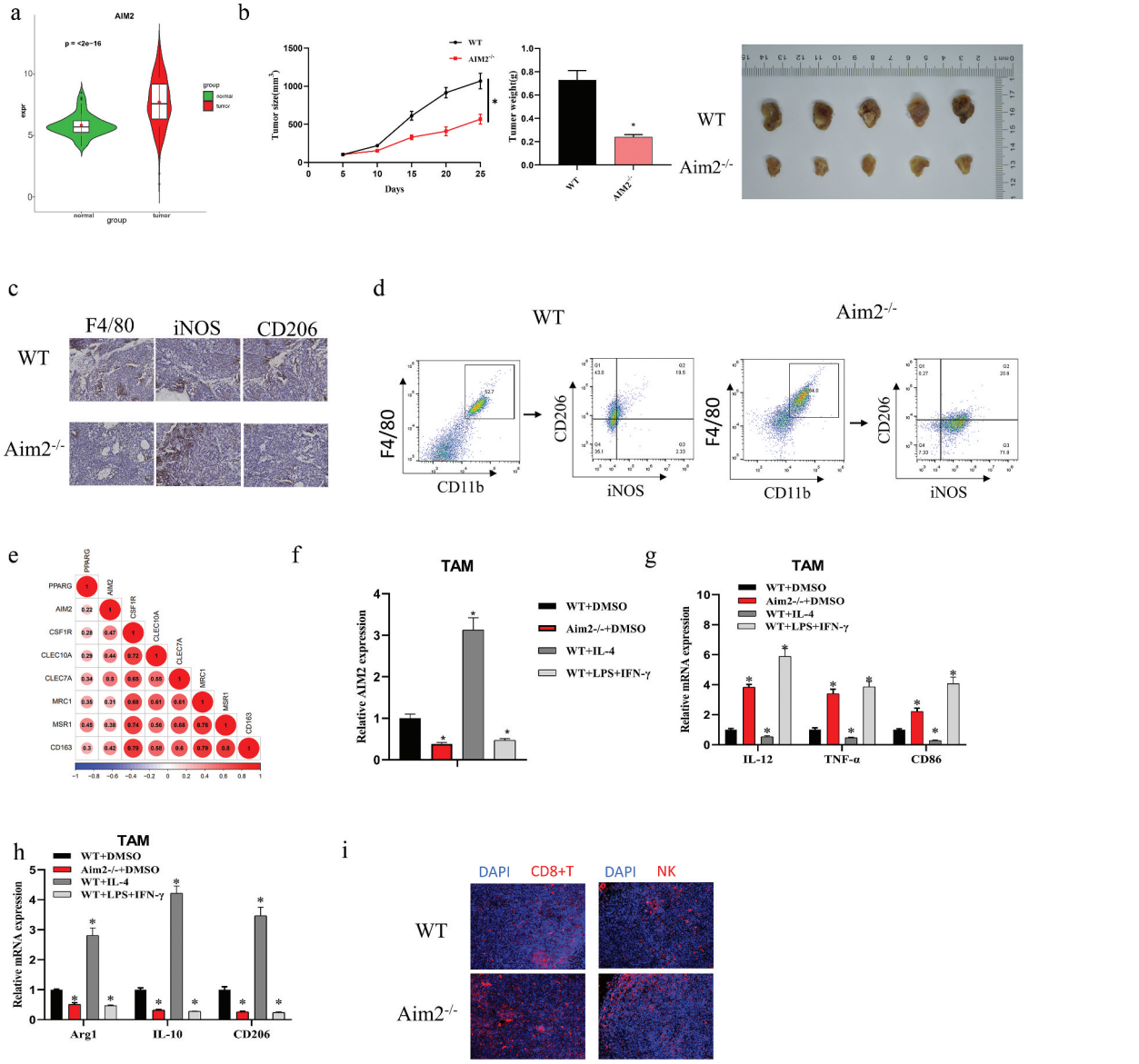

Figure 1. AIM2 fosters Mø to M2-type polarization. (a): AIM2 expression in LUAD tissues; (b): LUAD cell line LA795 was subcutaneously inoculated in mice ($n = 5$), and the tumor volume curve was drawn, and mice tumor images; (c): IHC was used to detect the expression of F4/80, iNOS and CD206 in LUAD tissue sections of mice treated with sh-AIM2; (d): The polarization of macrophages after sh-AIM2 treatment was detected by flow cytometry; (e): Bioinformatics analysis of the correlation between AIM2 and M2 Mø marker genes; (f-h): qPCR was used to detect the expression of AIM2, IL-12, TNF-α, CD86, Arg1, IL-10, and CD206; (i): The expression of $CD8^+$T cells and NK cells in tumor tissues of mice treated with sh-AIM2 was detected by IF. * indicates $P < .05$.

AIM2 affects LUAD growth, we purchased AIM2 knockout C57BL/6 mice (*Aim2*$^{-/-}$) and wild-type (WT) mice. Subsequently, LA795 cells were subcutaneously inoculated into the mice. It was observed that mice in the *Aim2*$^{-/-}$ group had slower tumor growth than the control group (Figure 1b). Flow cytometry and IHC results indicated a lower level of F4/80 Mø infiltration in *Aim2*$^{-/-}$ group (Figure 1c,d). Of note, *Aim2*$^{-/-}$ group had a high expression of the classic M1-type Mø marker iNOS, while low expression of the M2 Mø marker CD206 (Figure 1c,d). Therefore, we proposed the high expression of AIM2 in LUAD. Besides, AIM2 may promote Mø to M2-type polarization.

Next, to test this hypothesis, we identified M2-related genes through the literature[22] and conducted Pearson analysis between M2-related genes and AIM2, indicating a significant positive correlation between AIM2 expression and M2 Mø marker genes (Figure 1e). We then isolated macrophages from *Aim2*$^{-/-}$ mice and WT mice and treated them in groups: WT+DMSO, *Aim2*$^{-/-}$+DMSO, WT+IL-4, and WT+LPS+IFN-γ. As qPCR showed, the expression of AIM2 was tellingly downregulated in both the *Aim2*$^{-/-}$ group and the WT+LPS+IFN-γ group (induced to differentiate into M1 Mø) compared to the WT+DMSO group. However, in the WT+IL-4 group (induced to differentiate into M2 Mø), the expression of AIM2 was significantly upregulated (Figure 1f). In the *Aim2*$^{-/-}$+DMSO group and the WT+LPS+IFN-γ group, the expression of M1 Mø markers (IL-12, TNF-α, and CD86) was significantly upregulated, while the expression of M2 Mø marker genes (IL-10, Arg1, and CD206) was tellingly dropped. However, the WT +IL-4 group showed the opposite trend (Figure 1g,h). Furthermore, we also detected an apparent increase in the expression of immune cells, CD8^{+}T cells, and NK cells, in the *Aim2*$^{-/-}$ group through immunofluorescence (Figure 1i). The above experiments indicated that AIM2 could promote the Mø to M2-type polarization in LUAD.

AIM2 upregulates PD-L1 expression in M2 macrophages

We identified a notable positive association between AIM2 and PD-L1 expression by bioinformatics analysis (Figure 2a). AIM2 knockdown has previously been illustrated to facilitate the efficacy of anti-PD-L1 therapy.[17] Therefore, we examined the expression levels of PD-L1 in mouse macrophages. Through flow cytometry and ELISA, we discovered that the levels of PD-L1 in the *Aim2*$^{-/-}$ group were tellingly higher than those in the WT group (Figure 2b,c). Additionally, compared to the blank control and WT groups, we observed that the conditioned

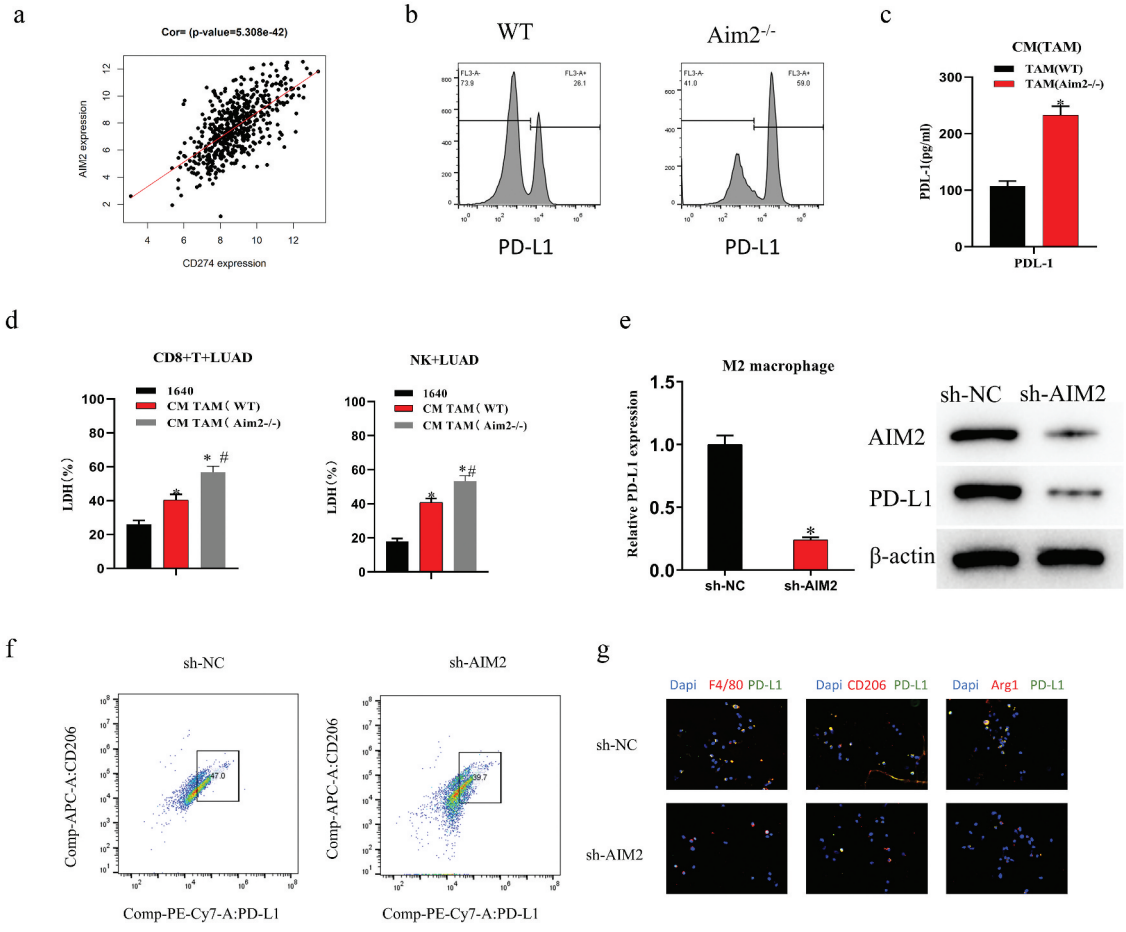

Figure 2. AIM2 upregulates PD-L1 expression in TAMs. (a): Bioinformatics analysis of the correlation between AIM2 and PD-L1; (b,c): The expression level of PD-L1 in WT and AIM2 groups was detected by flow cytometry and ELISA; (d): The cytotoxicity of CD8^{+}T cells and NK cells to LUAD cells was detected by LDH method; (e): qPCR and WB were used to detect PD-L1 expression in M2 Mø; (f): Proportion of CD206+PD-L1+ cells was detected by flow cytometry; (g): Multicolor IF was used to detect the expression of F4/80, CD206, Arg1, and their co-localization with PD-L1. * indicates $P < .05$.

medium (CM) from AIM2 knockout macrophages notably enhanced the cytotoxicity of $CD8^{+}$T cells and NK cells against LUAD cells (Figure 2d). To identify how AIM2 affects PD-L1 expression in M2 Mø, cell groups were subsequently constructed based on IL-4-induced M2 Mø: sh-NC and sh-AIM2. Based on qPCR and WB results, sh-AIM2 could tellingly reduce PD-L1 expression (Figure 2e). Moreover, sh-AIM2 treatment considerably decreased the ratio of CD206+PD-L1+ cells (Figure 2f). Finally, we detected the expression of Mø markers and their co-localization with PD-L1 by multicolor IF, with outcomes showing that the expression of Arg1, CD206, and F4/80 in the sh-AIM2 group was tellingly lower than that in the control group (Figure 2g), which was in line with IHC outcomes. Interestingly, PD-L1 was significantly co-localized with Arg1, CD206, and F4/80 in the control group (Figure 2g). The aforementioned investigations demonstrated that AIM2 possessed the capacity to notably enhance the upregulation of PD-L1 expression in TAMs.

AIM2 regulates M2 Mø polarization and upregulates PD-L1 expression via JAK/STAT3 signaling pathway

To further explore how AIM2 affected TAM polarization and PD-L1 expression, we first ascertained AIM2 enrichment in the JAK/STAT3 signaling pathway by bioinformatics analysis (Figure 3a). We then examined the expression of related proteins in the JAK/STAT pathway in AIM2-knockdown M2 Mø by WB. As expected, sh-AIM2 treatment lowered the phosphorylation levels of JAK1, STAT3, and JAK2, but had no effect on total JAK1, JAK2, or STAT3 (Figure 3b). To test this result, we performed rescue assay and constructed cell groups based on M2 Mø: oe-NC, oe-AIM2, and oe-AIM2+ AZD1480 (AZD1480 is a JAK inhibitor).[23] WB illustrated that oe-AIM2 could significantly drive the phosphorylation levels of STAT3, JAK1, and JAK2. Further treatment with AZD1480 reversed this effect (Figure 3c). oe-AIM2 promoted the expression of PDL1 and Arg1, and AZD1480 reversed the promoting effect of oe-AIM2 (Figure 3d). In conclusion, AIM2

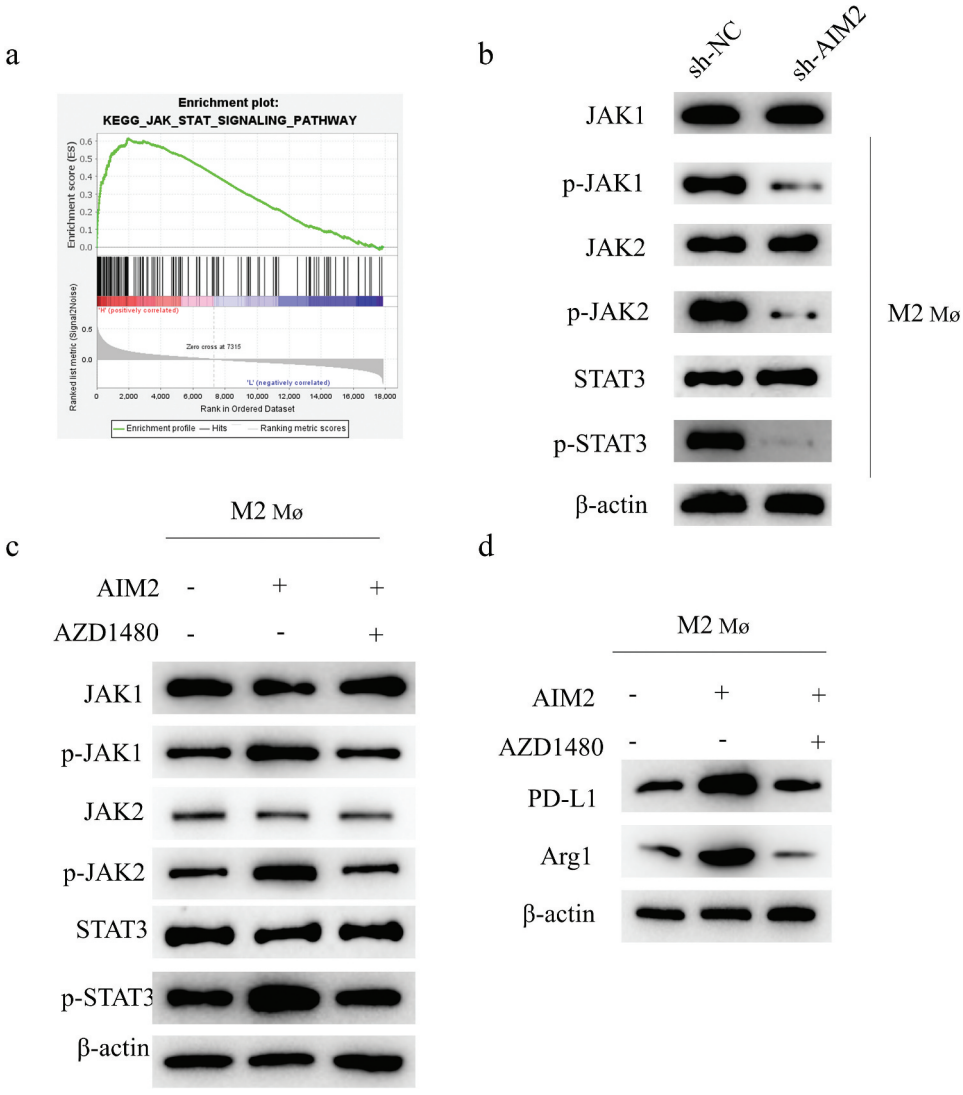

Figure 3. AIM2 regulates TAM polarization and upregulates PD-L1 expression via the JAK/STAT3 signaling pathway. (a): GSEA analysis showed that AIM2 was enriched on the JAK-STAT SIGNALING PATHWAY; (b,c): The expression and phosphorylation of JAK/STAT3 pathway-related proteins in different treatment groups were detected by WB; (d): WB analysis of PD-L1 and Arg1 expression in different treatment groups.

regulated M2 Mø polarization and upregulated PD-L1 expression via JAK/STAT3 signaling pathway.

AIM2 represses the immune infiltration of CD8$^+$T cells

To determine the cell types affected by AIM2 in tumor immune responses, we first evaluated CD4$^+$T, CD8$^+$T, and NK cell infiltration in tumor tissues of LUAD mice. As IHC results showed, sh-AIM2 treatment could significantly raise the infiltration level of CD8$^+$T cells. In contrast, infiltration levels of CD4$^+$T and NK cells were reduced (Figure 4a). Multicolor IF analysis of the co-localization of LUAD cells, Mø, M2 Mø, and PD-L1 with CD8$^+$T cells revealed a notable increase in the co-localization of CD8 with CK19 after sh-AIM2 treatment, indicating significant activation of CD8$^+$T cells (Figure 4b). From the above findings, AIM2 could inhibit the immune infiltration of CD8$^+$T cells in LUAD.

Reversal of AIM2 expression-induced immunosuppression in LUAD by PD-1/PD-L1 inhibitors

In TME, the binding of PD-1 and PD-L1 was to modulate T cell activation and repress T cell-mediated immune response.[24,25] Next, we explored the molecular mechanism of AIM2 inhibiting the immune function of CD8$^+$T cells in LUAD. IHC showed decreased PD-1 expression in LUAD tissues of mice after sh-AIM2 treatment (Figure 5a), and the co-localization level of PD-1 with PD-L1 was reduced (Figure 5b). We constructed cell groups based on M2 Mø: oe-NC+IgG, oe-AIM2+IgG, oe-AIM2+ anti-PD-L1, and oe-AIM2 + anti-PD-1, which were co-cultured with activated T cells, respectively. Then, the activation and proliferation levels of CD8$^+$T cells were assayed by flow cytometry, with outcomes revealing that oe-AIM2 significantly reduced the above levels of CD8$^+$T cells, which were reversed with the addition of PD-1 or PD-L1 antibodies to the culture system (Figure 5c,d). Based on the above outcomes, AIM2 exerted immunosuppressive effects via the PD-1/PD-L1 axis.

Discussion

The therapeutic influence of LUAD is unsatisfactory due to a lack of effective diagnosis and treatment.[26] In recent years, anti-tumor therapy for TME has attracted the attention of researchers. TAM weighs a lot in TME. M2 Mø represses the activation of CD8$^+$T cells via the PD-1/PD-L1 axis, thereby promoting tumor cell immune escape.[21,27] Here, we found for the first time the linkage between AIM2 and PD-L1 expression in LUAD Mø and demonstrated that AIM2 could foster M2 Mø polarization.

To date, M2 Mø features in tumor development have been proved by numerous studies. For example, overexpression of miR-21 in ovarian cancer was found by An et al.[28] to foster drug resistance and repress apoptosis of ovarian cancer cells by regulating M2 Mø polarization. Tu et al.[29] reported that M2 Mø can promote breast cancer cells to proliferate and migrate.

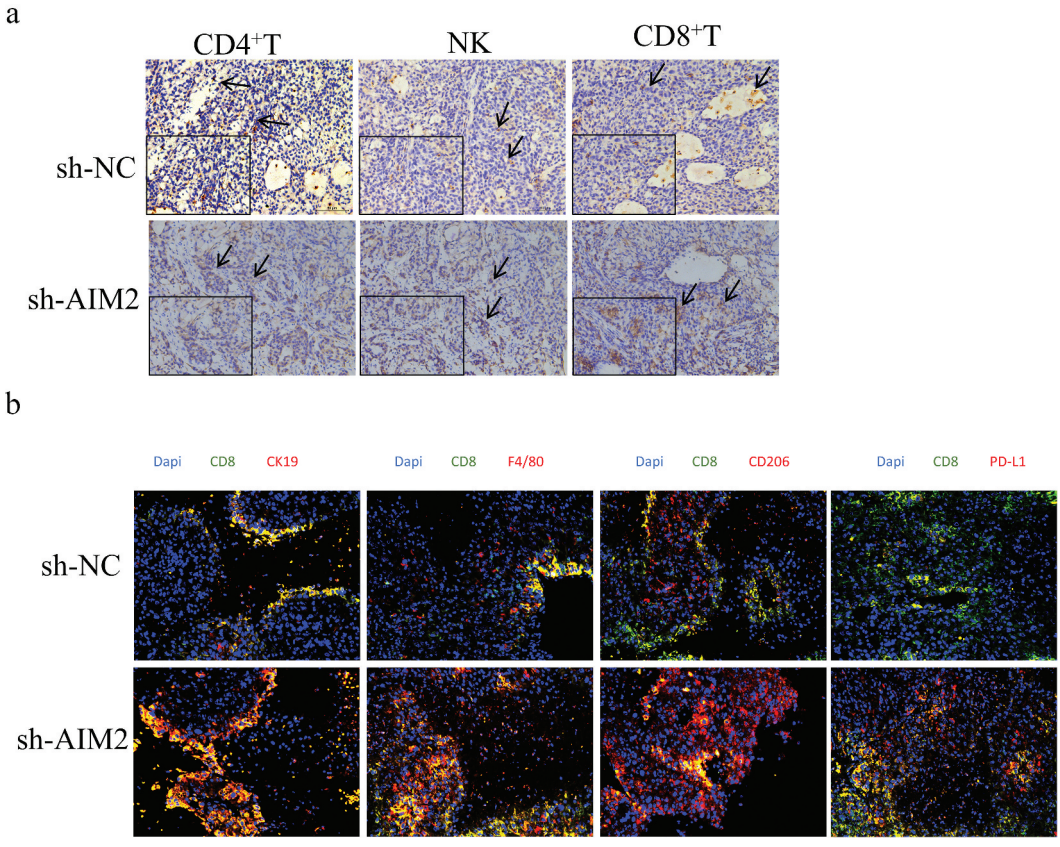

Figure 4. AIM2 represses the immune infiltration of CD8$^+$T cells. (a): The infiltration of CD4$^+$T, CD8$^+$T, and NK cells in different treatment groups was detected by IHC; (b): Multicolor IF was used to detect the co-localization of LUAD cells, Mø, M2 Mø, and PD-L1 with CD8$^+$T cells in different treatment groups.

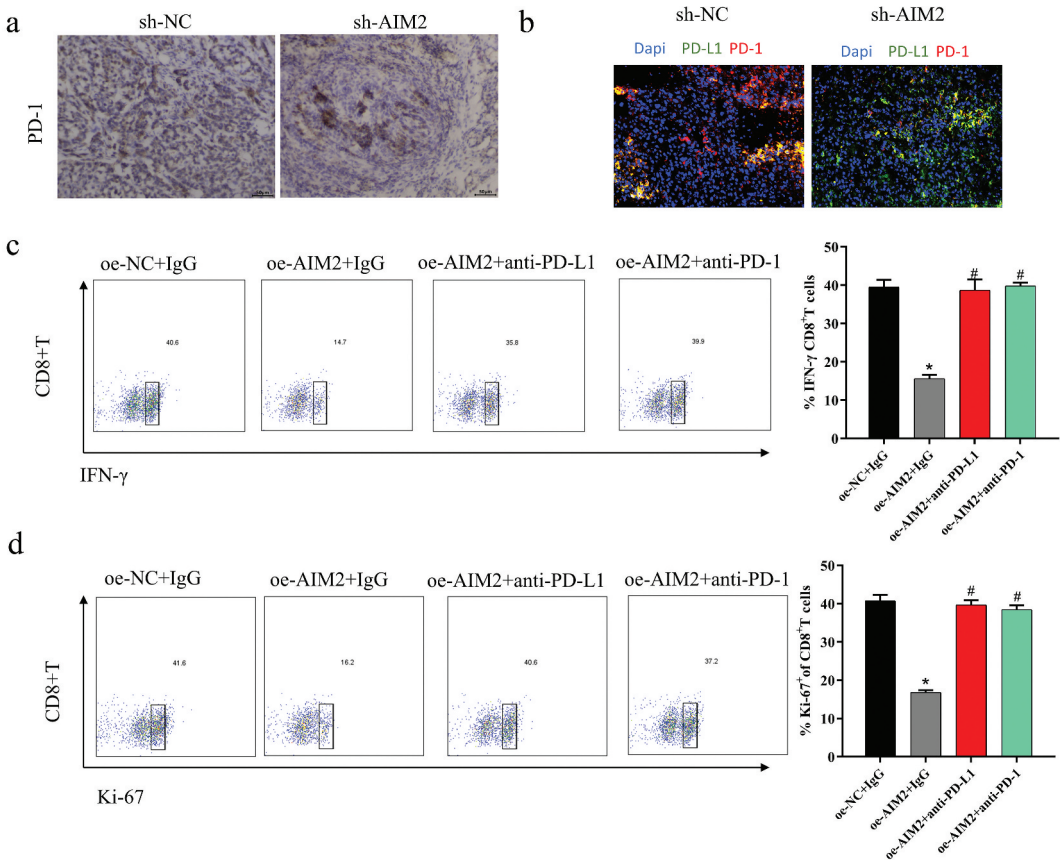

Figure 5. Reversal of AIM2 expression-induced immunosuppression in LUAD by PD-1/PD-L1 inhibitors. (a): PD-1 expression in LUAD tissues in different treatment groups was detected by IHC; (b): Multicolor fluorescence detection of PD-1 and PD-L1 co-localization in different treatment groups; (c,d): Activation and proliferation of $CD8^+$T cells in different treatment groups were detected by flow cytometry. *VS oe-NC+IgG; #VS oe-AIM2+IgG, */# indicates $P < .05$.

Additionally, the function of TAM in the process of tumor immune escape has been previously reported. For example, Ye et al.[30] revealed the significantly higher expression of lncRNA cox-2 in M1 Mø than in M2 Mø, and knockdown of cox-2 can promote M2 Mø polarization to promote immune escape and tumor growth in hepatocellular carcinoma. Human cytomegalovirus IE2 protein increases the expression of M2 Mø-linked cytokines IL-4 and IL-13 by up-regulating the expression of UL122, thereby promoting Mø-mediated immune escape.[31] This work found that high AIM2 expression in LUAD Mø promoted PD-L1 expression to repress immune infiltration of $CD8^+$T cells, thereby fostering tumor immune escape.

In accordance with the outcomes of bioinformatics analysis, a pronounced enrichment of AIM2 in the JAK/STAT3 signaling pathway was observed. Additionally, investigations into the relationship between AIM2 and the expression of STAT3 have been undertaken. IL-11 was reported to activate the transcription factor STAT3 to promote AIM2 expression.[32] The inflammasome AIM2 promotes intestinal homeostasis and reduces the risk of CRC via the IL-18/IL-22/STAT3 pathway.[33] It is well known that miscellaneous signaling pathways exist for the post-transcriptional modulation of PD-L1.[24,25] Of these signaling pathways, JAK/STAT/PI3K/AKT/MEK/ERK and SHP2/RAS/RAF/MEK/ERK pathways are the most important two.[34–36] We hypothesized that AIM2 regulated PD-L1 expression in Mø via JAK/STAT3. To this end, we used the inhibitor AZD1480 to block the JAK/STAT3 pathway. Phosphorylation levels of JAK1, JAK2, and STAT3 were found to be tellingly reduced, which suggested that AIM2 upregulated PD-L1 expression in Mø and fostered M2 Mø polarization by stimulating the JAK/STAT3 signaling pathway. Recent studies have shown that the AIM2 inflammasome pathway induces macrophage polarization toward an immunosuppressive phenotype by upregulating the expression of PD-L1 and indoleamine 2,3-dioxygenase (IDO). Blocking the AIM2 inflammasome can reduce the production of bioactive IL-1β and reverse the macrophage phenotype switch induced by CAR-T therapy.[37] Nonetheless, our research endeavors have thus far not encompassed the realms of chemokines and growth factors. Hence, we remain poised to embark on comprehensive investigations in these domains in the forthcoming stages.

Here, the linkage between AIM2 and PD-L1 expression in LUAD Mø was investigated for the first time. AIM2 was found to feature in promoting LUAD by modulating M2 Mø polarization and up-regulating PD-L1 expression through the JAK/STAT3 signaling pathway. Afterward, $CD8^+$T cell immune infiltration was repressed by PD-1/PD-L1 interaction. Hence, AIM2 can be a feasible target for immunotherapy of LUAD, and the clinical immunotherapy of LUAD can be more effective by targeting AIM2 combined with PD-1 antibody and PD-L1 antibody. However, shortcomings existed, we did not collect clinical LUAD samples to verify the accuracy of this study, and the direct influence of AIM2 on the PD-1/PD-L1 axis remains an enigma that necessitates further elucidation. At a later stage, we

will continue to explore whether there are genes downstream of AIM2 that affect PD-L1, and verify the experimental results by collecting tissues. Viewed in toto, our findings suggest AIM2 be a prospective clinical therapeutic target for LUAD.

Disclosure statement

No potential conflict of interest was reported by the author(s).

Funding

The author(s) reported there is no funding associated with the work featured in this article.

Author contribution

Conceptualization: Jifa Li; Data curation: Hua Ye; Formal Analysis: Wenwen Yu; Investigation: Yunlei Li; Methodology: Xiaoqiong Bao; Project administration: Jifa Li; Resources: Yangyang Ni; Software: Xiangxiang Chen; Supervision: Jifa Li; Validation: Yangjie Sun; Visualization: Ali Chen, Weilong Zhou; Writing – original draft: all the authors; Writing – review and editing: all the authors

Data availability statement

The data and materials in the current study are available from the corresponding author on reasonable request.

Ethics approval and consent to participate

This study was approved by the Ethics Committee of the Affiliated Yueqing Hospital of Wenzhou Medical University [YQYY202300004].

References

1. Wang J, Zhao X, Wang Y, Ren F, Sun D, Yan Y, Kong X, Bu J, Liu M, Xu S. circRNA-002178 act as a ceRNA to promote PDL1/PD1 expression in lung adenocarcinoma. Cell Death Disease. 2020;11(1):32. doi:10.1038/s41419-020-2230-9.
2. Chen Z, Huang Y, Hu Z, Zhao M, Li M, Bi G, Zheng Y, Liang J, Lu T, Jiang W, et al. Landscape and dynamics of single tumor and immune cells in early and advanced-stage lung adenocarcinoma. Clin Transl Med. 2021;11(3):e350. doi:10.1002/ctm2.350.
3. Hao J, Wang H, Song L, Li S, Che N, Zhang S, Zhang H, Wang J. Infiltration of CD8(+) FOXP3(+) T cells, CD8(+) T cells, and FOXP3 (+) T cells in non-small cell lung cancer microenvironment. Int J Clin Exp Pathol. 2020;13:880–8.
4. Fang W, Zhou T, Shi H, Yao M, Zhang D, Qian H, Zeng Q, Wang Y, Jin F, Chai C, et al. Progranulin induces immune escape in breast cancer via up-regulating PD-L1 expression on tumor-associated macrophages (TAMs) and promoting CD8(+) T cell exclusion. J Exp Clin Cancer Res. 2021;40(1):4. doi:10.1186/s13046-020-01786-6.
5. Essandoh K, Li Y, Huo J, Fan GC. MiRNA-Mediated macrophage polarization and its potential role in the regulation of inflammatory response. Shock. 2016;46(2):122–31. doi:10.1097/SHK.0000000000000604.
6. Rhee I. Diverse macrophages polarization in tumor microe nvironment. Arch Pharm Res. 2016;39(11):1588–96. doi:10.1007/s12272-016-0820-y.
7. Pello OM, De Pizzol M, Mirolo M, Soucek L, Zammataro L, Amabile A, Doni A, Nebuloni M, Swigart LB, Evan GI, et al. Role of c-MYC in alternative activation of human macrophages and tumor-associated macrophage biology. Blood. 2012;119 (2):411–21. doi:10.1182/blood-2011-02-339911.
8. Li S, Ding J, Wang Y, Wang X, Lv L. CD155/TIGIT signaling regulates the effector function of tumor-infiltrating CD8+ T cell by NF-kappaB pathway in colorectal cancer. J Gastroenterol Hepatol. 2022;37(1):154–63. doi:10.1111/jgh.15730.
9. Yan K, Fu Y, Zhu N, Wang Z, Hong JL, Li Y, Li WJ, Zhang HB, Song JH. Repression of lncRNA NEAT1 enhances the antitumor activity of CD8(+)T cells against hepatocellular carcinoma via regulating miR-155/Tim-3. Int J Biochem Cell Biol. 2019;110:1–8. doi:10.1016/j.biocel.2019.01.019.
10. Li H, Li Y, Song C, Hu Y, Dai M, Liu B, Pan P. Neutrophil extracellular traps augmented alveolar macrophage pyroptosis via AIM2 inflammasome activation in LPS-Induced ALI/ARDS. J Inflamm Res. 2021;14:4839–58. doi:10.2147/JIR.S321513.
11. Yang M, Long D, Hu L, Zhao Z, Li Q, Guo Y, He Z, Zhao M, Lu L, Li F, et al. AIM2 deficiency in B cells ameliorates systemic lupus erythematosus by regulating Blimp-1–Bcl-6 axis-mediated B-cell differentiation. Signal Transduct Target Ther. 2021;6(1):341. doi:10.1038/s41392-021-00725-x.
12. Lozano-Ruiz B, Gonzalez-Navajas JM. The emerging relevance of AIM2 in liver disease. Int J Mol Sci. 2020;21(18):6535. doi:10.3390/ijms21186535.
13. He B, Zhao Z, Cai Q, Zhang Y, Zhang P, Shi S, Xie H, Peng X, Yin W, Tao Y, et al. miRNA-based biomarkers, therapies, and resistance in cancer. Int J Biol Sci. 2020;16(14):2628–47. doi:10.7150/ijbs.47203.
14. Choubey D. Absent in melanoma 2 proteins in the development of cancer. Cell Mol Life Sci. 2016;73(23):4383–95. doi:10.1007/s00018-016-2296-9.
15. Xu M, Wang J, Li H, Zhang Z, Cheng Z. AIM2 inhibits colorectal cancer cell proliferation and migration through suppression of Gli1. Aging (Albany NY). 2020;13(1):1017–31. doi:10.18632/aging.202226.
16. Li Y, Wang W, Li A, Huang W, Chen S, Han F, Wang L. Dihydroartemisinin induces pyroptosis by promoting the AIM2/caspase-3/DFNA5 axis in breast cancer cells. Chem Biol Interact. 2021;340:109434. doi:10.1016/j.cbi.2021.109434.
17. Fukuda K, Okamura K, Riding RL, Fan X, Afshari K, Haddadi NS, McCauley SM, Guney MH, Luban J, Funakoshi T, et al. AIM2 regulates anti-tumor immunity and is a viable therapeutic target for melanoma. J Exp Med. 2021;218(9). doi:10.1084/jem.20200962.
18. Su S, Zhao J, Xing Y, Zhang X, Liu J, Ouyang Q, Chen J, Su F, Liu Q, Song E. Immune checkpoint inhibition overcomes ADCP-Induced immunosuppression by macrophages. Cell. 2018;175(2):442–57 e23. doi:10.1016/j.cell.2018.09.007.
19. Shi S, Ma B, Sun F, Qu C, Li G, Shi D, Liu W, Zhang H, An H. Zafirlukast inhibits the growth of lung adenocarcinoma via inhibiting TMEM16A channel activity. J Biol Chem. 2022;298 (3):101731. doi:10.1016/j.jbc.2022.101731.
20. Hou Y, Zhu L, Tian H, Sun HX, Wang R, Zhang L, Zhao Y. IL-23-induced macrophage polarization and its pathological roles in mice with imiquimod-induced psoriasis. Protein Cell. 2018;9 (12):1027–38. doi:10.1007/s13238-018-0505-z.
21. Dai X, Lu L, Deng S, Meng J, Wan C, Huang J, Sun Y, Hu Y, Wu B, Wu G, et al. USP7 targeting modulates anti-tumor immune response by reprogramming tumor-associated macrophages in lung cancer. Theranostics. 2020;10(20):9332–47. doi:10.7150/thno.47137.
22. Oliveira LJ, McClellan S, Hansen PJ, Kaul R. Differentiation of the endometrial macrophage during pregnancy in the cow. PloS One. 2010;5(10):e13213. doi:10.1371/journal.pone.0013213.
23. Wang T, Fahrmann JF, Lee H, Li YJ, Tripathi SC, Yue C, Zhang C, Lifshitz V, Song J, Yuan Y, et al. JAK/STAT3-regulated fatty acid β-oxidation is Critical for breast cancer stem cell self-renewal and Chemoresistance. Cell Metabolism. 2018;27(1):136–50 e5. doi:10.1016/j.cmet.2017.11.001.
24. Sun C, Mezzadra R, Schumacher TN. Regulation and function of the PD-L1 checkpoint. Immunity. 2018;48(3):434–52. doi:10.1016/j.immuni.2018.03.014.
25. Francisco LM, Sage PT, Sharpe AH. The PD-1 pathway in tolerance and autoimmunity. Immunol Rev. 2010;236(1):219–42. doi:10.1111/j.1600-065X.2010.00923.x.

26. Wang Y. Circ-ANXA7 facilitates lung adenocarcinoma progression via miR-331/LAD1 axis. Cancer Cell Int. 2021;21(1):85. doi:10.1186/s12935-021-01791-5.
27. Feng M, Jiang W, Kim BYS, Zhang CC, Fu YX, Weissman IL. Phagocytosis checkpoints as new targets for cancer immunotherapy. Nat Rev Cancer. 2019;19(10):568–86. doi:10.1038/s41568-019-0183-z.
28. Pasaoglu A, Patiroglu TE, Orhon C, Yildizhan A. Cervical spinal intramedullary myxoma in childhood: case report. J Neurosurg. 1988;69(5):772–4. doi:10.3171/jns.1988.69.5.0772.
29. Tu D, Dou J, Wang M, Zhuang H, Zhang X. M2 macrophages contribute to cell proliferation and migration of breast cancer. Cell Biol Int. 2021;45(4):831–8. doi:10.1002/cbin.11528.
30. Ye Y, Xu Y, Lai Y, He W, Li Y, Wang R, Luo X, Chen R, Chen T. Long non-coding RNA cox-2 prevents immune evasion and metastasis of hepatocellular carcinoma by altering M1/M2 macrophage polarization. J Cell Biochem. 2018;119(3):2951–63. doi:10.1002/jcb.26509.
31. Yang Y, Ren G, Wang Z, Wang B. Human cytomegalovirus IE2 protein regulates macrophage-mediated immune escape by upregulating GRB2 expression in UL122 genetically modified mice. Biosci Trends. 2020;13(6):502–9. doi:10.5582/bst.2019.01197.
32. Dawson RE, Deswaerte V, West AC, Tang K, West AJ, Balic JJ, Gearing LJ, Saad MI, Yu L, Wu Y, et al. STAT3-mediated upregulation of the AIM2 DNA sensor links innate immunity with cell migration to promote epithelial tumourigenesis. Gut. 2022;71(8):1515–31. doi:10.1136/gutjnl-2020-323916.
33. Ratsimandresey RA, Indramohan M, Dorfleutner A, Stehlik C. The AIM2 inflammasome is a central regulator of intestinal homeostasis through the IL-18/IL-22/STAT3 pathway. Cell Mol Immunol. 2017;14(1):127–42. doi:10.1038/cmi.2016.35.
34. Zhang X, Zeng Y, Qu Q, Zhu J, Liu Z, Ning W, Zeng H, Zhang N, Du W, Chen C, et al. PD-L1 induced by IFN-γ from tumor-associated macrophages via the JAK/STAT3 and PI3K/AKT signaling pathways promoted progression of lung cancer. Int J Clin Oncol. 2017;22(6):1026–33. doi:10.1007/s10147-017-1161-7.
35. Qiu XY, Hu DX, Chen WQ, Chen RQ, Qian SR, Li CY, Li YJ, Xiong XX, Liu D, Pan F, et al. PD-L1 confers glioblastoma multiforme malignancy via Ras binding and Ras/Erk/EMT activation. Biochim Biophys Acta Mol Basis Dis. 2018;1864(5):1754–69. doi:10.1016/j.bbadis.2018.03.002.
36. Li P, Huang T, Zou Q, Liu D, Wang Y, Tan X, Wei Y, Qiu H. FGFR2 promotes expression of PD-L1 in colorectal cancer via the JAK/STAT3 signaling pathway. J Immunol. 2019;202(10):3065–75. doi:10.4049/jimmunol.1801199.
37. Liu D, Xu X, Dai Y, Zhao X, Bao S, Ma W, Zha L, Liu S, Liu Y, Zheng J, et al. Blockade of AIM2 inflammasome or α1-AR ameliorates IL-1β release and macrophage-mediated immunosuppression induced by CAR-T treatment. J Immunother Cancer. 2021;9(1):e001466. doi:10.1136/jitc-2020-001466.